Anoxia stimulates microbially catalyzed metal release from Animas River sediments

6 authors, including:

Casey Saup
The Ohio State University

4 PUBLICATIONS   **1** CITATION

SEE PROFILE

José M Cerrato
University of New Mexico

38 PUBLICATIONS   **500** CITATIONS

SEE PROFILE

Some of the authors of this publication are also working on these related projects:

The role of microorganisms in the biogeochemical cycle of arsenic View project

Animas river View project

PAPER

CrossMark
click for updates

Anoxia stimulates microbially catalyzed metal release from Animas River sediments†

Casey M. Saup,[a] Kenneth H. Williams,[b] Lucía Rodríguez-Freire,[c] José M. Cerrato,[c] Michael D. Johnston[a] and Michael J. Wilkins*[ad]

The Gold King Mine spill in August 2015 released 11 million liters of metal-rich mine waste to the Animas River watershed, an area that has been previously exposed to historical mining activity spanning more than a century. Although adsorption onto fluvial sediments was responsible for rapid immobilization of a significant fraction of the spill-associated metals, patterns of longer-term mobility are poorly constrained. Metals associated with river sediments collected downstream of the Gold King Mine in August 2015 exhibited distinct presence and abundance patterns linked to location and mineralogy. Simulating riverbed burial and development of anoxic conditions, sediment microcosm experiments amended with Animas River dissolved organic carbon revealed the release of specific metal pools coupled to microbial Fe- and SO_4^{2-}-reduction. Results suggest that future sedimentation and burial of riverbed materials may drive longer-term changes in patterns of metal remobilization linked to anaerobic microbial metabolism, potentially driving decreases in downstream water quality. Such patterns emphasize the need for long-term water monitoring efforts in metal-impacted watersheds.

Environmental impact

Historical mining activities have impacted environmental systems throughout the world through the release of waste products and contaminants. The waste spill in August 2015 at the Gold King Mine in Colorado into the Animas River has raised concerns about long-term patterns of metal fate and transport in this watershed. Here, we demonstrate specific patterns of contaminant metal remobilization from fluvial sediments by anaerobic microbial metabolism. These results highlight the importance of long-term monitoring of river water quality as metal-hosted river sediments undergo burial processes that lead to development of anoxic conditions that favor metal release.

Introduction

Mining activities impact hydrologic systems across the globe, either through the release of waste products, or through long-term leaching of contaminants following mine abandonment. Globally, costs of mine waste remediation are estimated to be in the tens of billions of dollars.[1] In western Colorado, such problems have contributed to approximately 40% of streams representing a risk to human and ecosystem health.[2] The Animas River in southern Colorado begins in the San Juan Mountains and subsequently flows through New Mexico before

discharging into the San Juan River. S and metal-rich hydrothermal fluids have previously contributed to high abundances of metal-sulfide minerals in this surrounding area. Weathering of these phases has removed the acid buffering capacity associated with the original calcite–chlorite–epidote mineralogy, contributing to lower pH and elevated trace metal concentrations in localized riverine systems.[3] Combined with historical mining activities within this watershed over the past 100 years,[2] these processes have generated elevated concentrations of various heavy metals including Al, Cd, Cu, Pb, and Mn in fluvial sediments and river water itself.[3] Supplementing a legacy of mining and milling impacts in the area, punctuated events, such as the Gold King Mine spill in August 2015, have the potential to contribute sizable inputs of heavy metals to the watershed over very short time intervals.[4]

While metals in river water may become rapidly diluted, a significant fraction may be removed from the water column through sorption reactions on reactive grain coatings in riverbed sediments.[5] Under oxic conditions this represents an immobilized contaminant pool that poses a decreased risk to downstream water quality.[6] Over time, however, the burial of fluvial sediments drives the onset of sub-oxic and anoxic

[a]School of Earth Sciences, The Ohio State University, 275 Mendenhall Laboratory, 125 South Oval Mall, Columbus, OH 43210, USA. E-mail: wilkins.231@osu.edu

[b]Earth & Environmental Sciences, Lawrence Berkeley National Lab, 1 Cyclotron Road, MS74R316C, Berkeley, CA 94720, USA

[c]Department of Civil Engineering, University of New Mexico, MSC01 10701, Albuquerque, NM 87131, USA

[d]Microbiology Department, The Ohio State University, 105 Biological Sciences Building, 484 W. 12th Ave, Columbus, OH 43210, USA

† Electronic supplementary information (ESI) available. See DOI: 10.1039/c7em00036g

conditions in the riverbed, where a range of microbial processes may cause the reductive dissolution of reactive Fe^{3+} and Mn^{4+} grain coatings[7,8] that are frequently associated with other metals.[9,10] Microbes may directly reduce and dissolve Fe^{3+} and Mn^{4+} coatings,[11] while biogenic S^{2-} (produced via microbial SO_4^{2-} reduction) can abiotically catalyze the same process.[12] Groundwater in much of the Colorado Basin has naturally elevated levels of SO_4^{2-} due to the weathering and leaching of pyritic shales and gypsum-rich evaporites, respectively,[13] and oxidation of metal sulfide-rich ore deposits[14] within mineralized rock, with SO_4^{2-} entering river channels via groundwater discharge and hyporheic exchange.[15] Regardless of mechanism, the reductive dissolution of reactive Fe^{3+} and Mn^{4+} grain coatings can lead to the release of co-associated metals into the aqueous phase,[7,8] with subsequent implications for downstream water chemistry and long-term monitoring plans for watersheds such as the Animas River. The objective of this study was to determine the effects of anaerobic microbial metabolism on Animas River sediment biogeochemistry, with particular emphasis on identifying drivers of long term heavy metal (re)mobilization. Following the Gold King Mine spill in August 2015, we collected near-surface sediments from three locations along the Animas River to assess patterns of metal release from sediments incubated under anoxic conditions in anaerobic batch incubations. Both dissolved organic carbon (DOC) present in river water and exogenous acetate stimulated the generation of reduced, redox active species and concurrent release of trace metals over a 28 day period. However, differing sediment mineralogy between the three locations resulted in varying patterns of metal release into the aqueous phase. These results are broadly relevant for the determination of biogeochemical processes affecting the long-term release of metals, particularly metal fate and transport, from contaminated fluvial sediments in rivers impaired by mining activities.

Methods

Sample collection

100 g of sediment near-surface grab-samples were collected from 3 riverbank locations along the Animas River: the USGS stream gauging station in Silverton, referred to here as A72 (37.790567, -107.667503); the City of Durango's Oxbow Park and Preserve (37.308843, -107.853842); and the 32nd St. Bridge in Durango (37.300072, -107.868922). Sediments were collected aseptically, stored in sterile Mylar bags, and shipped overnight to The Ohio State University (OSU) and the University of New Mexico (UNM) on blue ice. Samples were hand-homogenized in the lab to ensure consistency.

Metal extraction

Sediment samples were dried overnight at 60 °C and crushed to a fine powder. One gram of the pulverized sediment was digested with 3 mL and 2 mL of trace metals grade, concentrated HCl and HNO_3, respectively, and heated in a Digi prep MS SCP Science block digester at 90 °C for 2 hours. The digested sediment samples were filtered through 0.45 μm filters (25 mm

PTFE Membrane syringe filter) prior to analyses. The filtrate was analysed at the UNM Analytical Chemistry Laboratory using inductively coupled plasma ionization (ICP) coupled with either an optical emission spectrometer (ICP-OES, PerkinElmer Optima 5300DV with a detection limit of <0.01 mg L^{-1}) or a mass spectrometer (ICP-MS, PerkinElmer NexION 300D, with a detection limit of <0.5 μg L^{-1}).

Solid characterization analyses

Samples from each location at 0 days and after 28 days from each microcosm carbon treatment were dried overnight at 60 °C and ground by hand using a mortar and pestle. Sediment was back-loaded as a powder into a randomly oriented zero-background mount and analysed using X-ray diffractometry (XRD). The PANalytical X'Pert Pro XRD in the Subsurface Energy Materials Characterization & Analysis Laboratory (SEMCAL) in the School of Earth Sciences at The Ohio State University was used for analysis. Samples were scanned using Ni-filtered CuKα radiation. A step size of 0.020° 2θ was used from 4.0–70.0° at 2 s per step. Tension was set to 45 kV and current to 40 mA. Incident beam optics were 1, 2 and diffracted beam optics were 2, 1. To determine background, the PANalytical HighScore (Plus) program and Data Viewer were used with a granularity of 20 and a bending factor of 2. Peaks were searched with a minimum significance of 1.00, minimum tip width of 0.10, maximum tip width of 1.00, and peak base width of 2.00. After the automated search was complete, unmarked peaks were inserted manually. The Search and Match feature of HighScore (Plus) was used to determine mineralogical composition of the sediments.

Sediments from location A72 were dried overnight at 60 °C and analysed at the UNM Center for Micro-Engineered Materials facilities using an X-ray Photoelectron Spectrometer (XPS, Kratos AXIS-UltraDLD) to acquire the near surface (5–10 nm) elemental composition and Fe oxidation states. The source used was a monochromatic Al Kα 225 W. Each sample was scanned in triplicate and the presented data is the average of the three areas. Low energy electrons at standard operating conditions of −3.1 V bias voltage, 1.0 V filament voltage and filament current of 2.1 A were used for charge compensation. Gold powder was deposited on each sample, and Au 4f spectra were acquired for calibration purposes. All spectra were charge referenced to Au 4f at 84 eV. The spectra were processed using CasaXPS. Atomic percentage content was calculated using sensitivity factors provided by the manufacturer. A 70% Gaussian/30% Lorentzian (GL (30)) line shape was used for the curve-fits.

Microcosm experiments

Each microcosm consisted of 20 g of wet sediment from the appropriate location with 50 mL of river water (DOC concentration of ~2.75 mg L^{-1}) collected from the 32nd St. Bridge location in an anaerobic serum vial (headspace 95% N_2 and 5% CO_2). Microcosms were either provided with natural DOC (final concentration of added DOC 0.45 mg L^{-1}), which was enriched from river water, or acetate (positive control, 820 mg L^{-1}). DOC was concentrated from 20 L of Animas River water from the 32nd St. Bridge location using Agilent Bond Elute PPL columns

(Agilent Technologies, Santa Clara, CA, USA), methanol as the column eluent, and sterile deionized water as the final solvent. A negative control microcosm for each sediment sample did not receive additional DOC. Microcosms were incubated at room temperature in the dark. Temporal sediment–water samples were recovered biweekly from each microcosm during a 28 day period in aliquots of 3 mL using a 3 mL syringe fitted with an 21G needle. After 20 days, exogenous SO_4^{2-} (15 mM) was added to each microcosm to stimulate additional SO_4^{2-} reduction. Aqueous Fe and S^{2-} were measured using colorimetric methods (ferrozine and methylene blue assays, respectively), while sediment–water slurries were used for total DNA extractions (MoBio Powersoil DNA extraction kit, MoBio, CA, USA). Sediment–water slurries were centrifuged and the supernatant was filtered through a 0.22 μm filter and preserved for ICP-MS and ion chromatography (IC) analyses. Anions (acetate, SO_4^{2-}) were analysed using a Dionex ICS-2100 ion chromatograph at OSU. Detection limits for the anions were 0.1 mM and 0.01 mM, respectively. ICP-MS analyses for aqueous metal concentrations (Sr, Hg, Mo, Zn, Fe, As, Pb) were performed at OSU using a PerkinElmer ELAN 6000 Inductively Coupled Plasma Mass Spectrometer. 16S rRNA genes in extracted DNA were sequenced at Argonne National Laboratory using bacterial/archaeal primer set 515F/806R that targets the V4 region and maximizes coverage of bacteria and archaea while also providing polymerase chain reaction (PCR) products long enough for sequencing.[16] Resulting reads were checked for chimeras (USEARCH 61 algorithm) and subsequently clustered into operational taxonomic unit (OTU) classifications at 97% similarities (open-reference picking) using the QIIME pipeline (V1.7.0) and SILVA 16S rRNA database.[17] Subsequent analyses were performed using the R vegan package to determine linkages between geochemical variables and temporal microbial changes. Sequences are deposited at the NCBI Sequence Read Archive under accession number PRJNA321191.

Results & discussion

Solid characterization analyses

X-Ray diffraction (XRD) analyses revealed that sediments from the A72 site, which had a visible orange color and were more fine-grained than materials from the other two locations, contained a higher proportion of both clay and Fe-bearing minerals in the forms of illite, lepidocrocite, chamosite, and jarosite, a mineral commonly associated with Fe-rich acid mine waste. Sediments from the 32nd St. Bridge and Oxbow Park locations were dominated by igneous and metamorphic minerals and their weathering products (*e.g.*, amphiboles, zeolites). Following the 28 day incubation, there is a decrease in the abundance of sedimentary lepidocrocite and jarosite (ESI†). Total metal extractions were performed on each sediment type, offering insights into the linkages between differences in mineralogy and sample location to metal loadings. Bulk A72 sediments contained greater quantities of As, Cu, Mo, Pb, Sr, and Hg than the other two locations, potentially reflecting proximity of this location to contaminant point sources (*e.g.*, the Gold King Mine and innumerable other mines within the Silverton, CO area) (Fig. 1). Analyses of high resolution XPS (preformed only on A72 sediments) Fe 3p spectra

Fig. 1 Terrain/satellite view of the study site. Stars indicate sampling locations and the red circle indicates the location of the Gold King Mine.

from the near-surface region of the sediments from sample A72 indicated the presence of 52.3% Fe^{2+} and 47.7% Fe^{3+}. Fitting of XPS high resolution spectra suggest that Pb^{2+}, SO_4^{2-} and PO_4^{3-} are present in these sediments (Table 1 and Fig. 2). The presence of Zn was also detected at an atomic content of 0.04% Zn 2p according to the XPS survey scan. Bulk sediments from further downstream locations – the 32nd St. Bridge and Oxbow Park sampling sites, 73 km and 75 km from A72, respectively – generally showed similar trends to each other, and contained higher quantities of Zn, Co, Cd, Cr than materials from the A72 site (Fig. 3).

Carbon stimulated microbial activity

Over time, fluvial deposition can result in the burial of near-surface sediments and associated organic carbon, inducing the development of anoxic conditions.[6] To determine how such processes could contribute to changes in metal mobility, sediment microcosms were incubated under a range of carbon loadings and sampled for geochemical and microbiological parameters. All incubations induced biogeochemical changes, with generally similar geochemical trends irrespective of carbon addition or carbon addition type (DOC replicates *vs.* acetate positive control) (Fig. 4). Activity observed in microcosms that received no additional carbon indicates that labile sediment-associated organic substrates were available and capable of stimulating microbial metabolism. Higher concentrations of bioavailable Fe^{3+}-oxy-hydroxides in A72 materials supported microbial Fe reduction, as inferred from accumulation of Fe^{2+} in microcosm fluids. This is further supported by the decrease in the abundance of sedimentary lepidocrocite and jarosite observed in XPS data following the 28 day experiment which suggests that these minerals were available for microbial reduction (see ESI†). Although no clear

**Table 1** Metal speciation in the sediments using X-ray photoelectron spectroscopy (XPS)

| Sampling location	% content									
	Al 2p	Si 2p	Mg KLL	N 1s	Na 1s	P 2p	Pb 4f	Zn 2p	Fe^{2+}	Fe^{3+}
A72	30.6	47.3	1.4	2.9	1.4	0.71	0.13	0.04	52.3	47.7

trends in dissolved Fe concentrations were apparent in Oxbow Park and 32nd St. Bridge microcosms over the experiment, decreases in aqueous SO_4^{2-} concentrations (Oxbow Park – $\sim$500 μM; 32nd St. Bridge – $\sim$2 mM) are indicative of ongoing SO_4^{2-} reduction over the first three weeks of the incubation. A small increase ($\sim$2 mM) in the A72 microcosms is likely the result of the dissolution of the jarosite $(KFe(III)_3(OH)_6(SO_4)_2)$ mineral group that was identified in these sediments following the spill (ESI†). Rapid SO_4^{2-} reduction was observed in all microcosms following the addition of exogenous SO_4^{2-} at day 21 to stimulate microbial activity, with concurrent increases in measurable aqueous S^{2-} (Fig. 4).

Patterns of metal mobilization

Metal release was seemingly independent of bulk sediment metal concentration. The only metal mobilized in materials from the A72 locations was Zn, which was identified via XPS as co-occurring with Fe in near-surface sediment regions (Table 1). This observation supports the inference that anoxic biogeochemical processes at the mineral–water interface caused the release of Zn and Fe to solution, as the most near-surface Fe grain coatings which contain the Zn (Table 1) would be the first to solubilize. Zn concentrations did not increase in sediments receiving acetate as a carbon substrate (Fig. 4). This lack of Zn
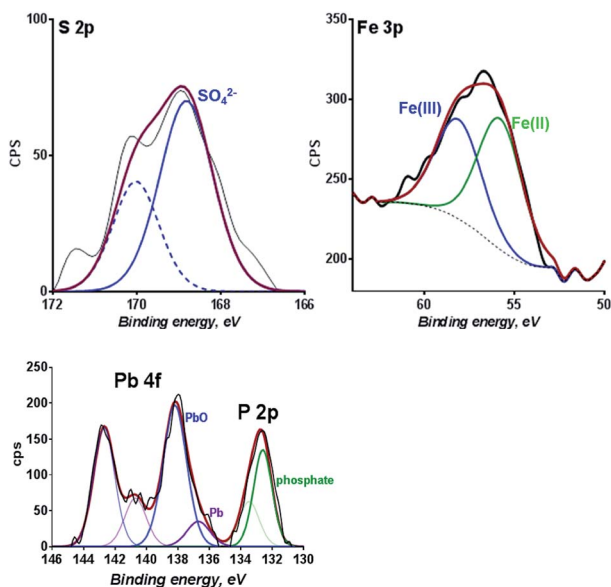
Fig. 2 X-ray photoelectron spectra (XPS) for the sediment sample location A72 for the elements S (S 2p), Fe (Fe 3p), Pb (Pb 4f), and P (P 2p).
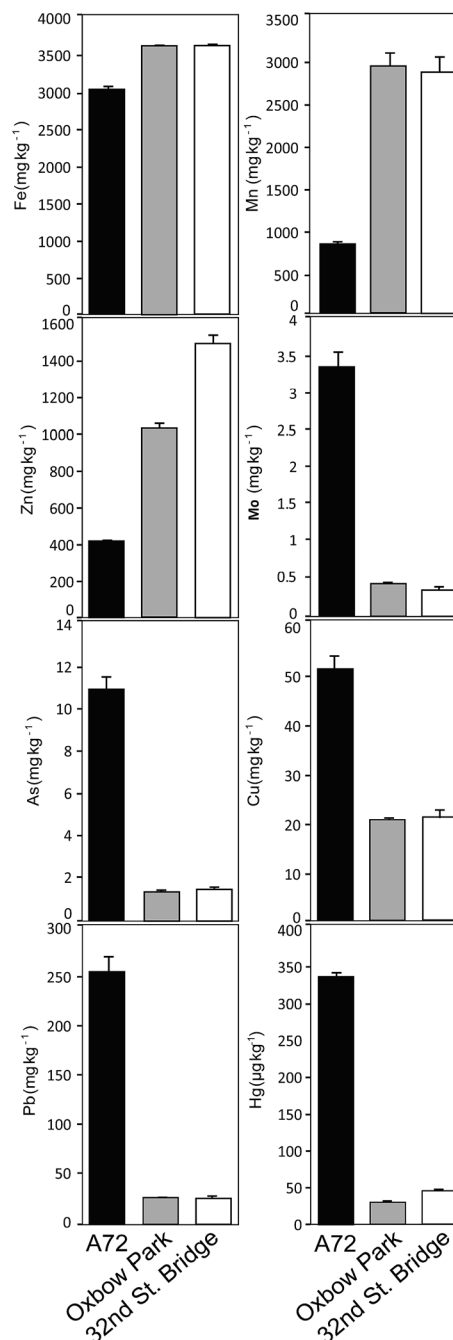
Fig. 3 Metal concentrations extracted from near-surface fluvial sediments from each site. Quantities represented in mg metals per kg sediments.
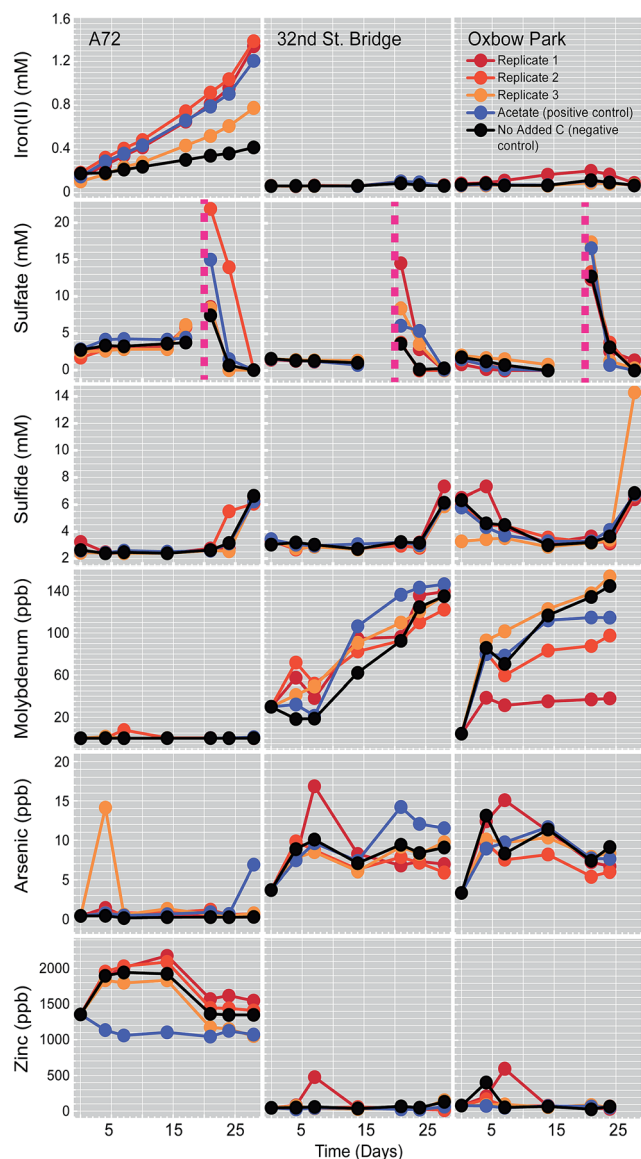
Fig. 4 Concentration changes in aqueous metal cations and anions from the three sediment types across 28 day microcosm incubations. The dashed line in the SO_4^{2-} panel indicates the time point where exogenous SO_4^{2-} was added to microcosms to stimulate additional SO_4^{2-} reduction.

For example, Pb is generally more competitive than Cu, Cd, and Zn in sorption to clay minerals and is therefore less likely to be released during development of anoxic conditions.[20] Clays, such as the illites observed in our XRD analyses (ESI†) and organo-clay complexes generally have a net negative charge, and therefore a relatively high cation exchange capacity, which allows for the electrostatic attraction and subsequent adsorption of heavy metal cations.[21–23] Although aqueous As and Mo concentrations showed little change in A72 materials, increases were observed in fluids from both Oxbow Park and 32nd St. Bridge sediment microcosms, concurrent with inferred SO_4^{2-} reduction and increasingly reduced conditions (Fig. 4). Aqueous Mo concentrations generally increased by over 100 ppb over the course of the experiment, while aqueous As concentrations rapidly increased by approximately 5–10 ppb before showing some minor decreases. Mo adsorption is strongly pH dependent, with more basic conditions favoring desorption from sediment facies.[24] Given that enzymatic SO_4^{2-} reduction generates significant alkalinity increases,[25] the greater extent of this process in the Oxbow Park and 32nd St. Bridge microcosms may have resulted in release of Mo. Although the precipitation of MoS_2 and adsorption of Mo onto Fe–S minerals may drive reductions in metal mobility over geologic time scales, many aqueous intermediate forms (e.g., thiomolybdate species) exist across smaller time scales and generally do not precipitate spontaneously.[26] Similar processes could have accounted for patterns of As release (and formation of thioarsenate species) in the same microcosms (Fig. 4), supporting observations made in similar alluvial sediments under sulfidic conditions.[8,27] SO_4^{2-} reduction caused a ∼1–3 mM decrease in the concentration of aqueous SO_4^{2-}, a trend which becomes much more dramatic (increased rate) following the addition of exogenous SO_4^{2-} at day 21 to stimulate additional SO_4^{2-} reduction. Although pH sampling was not feasible in this particular experiment, the ∼1–3 mM decrease in SO_4^{2-} via SO_4^{2-} reduction is expected to generate slight increases in alkalinity, likely enabling the release of As and Mo from sediments. Additionally, the apparent differences in rates of SO_4^{2-} reduction and As and Mo release could be caused by the formation of poorly crystalline sulfide minerals. No clear trends were observed across any of the microcosms for additional metal species (see ESI†).

Microbial community dynamics

16S rRNA genes were examined via non-metric multidimensional scaling (NMDS, an ordination plot) for emergent properties using R v3.3.2 (metaMDS). Differences identified via NMDS were compared using an analysis of similarities (ANOSIM) (anosim, vegan package v.2.4-2 (ref. 28)). To identify putative geochemical (Fig. 5) and microbial (Fig. 6) drivers of shifts in microbial community structure, correlative relationships were determined using a Mantel Test (mantel, vegan package v.2.4-2 (ref. 28)) followed by a more thorough examination in a canonical correspondence analysis (CCA) (vegan package v.2.4-2 (ref. 28)). In an NMDS plot, the distance between each of the plotted points (which represents a snapshot of the microbial community from a specific time point in each
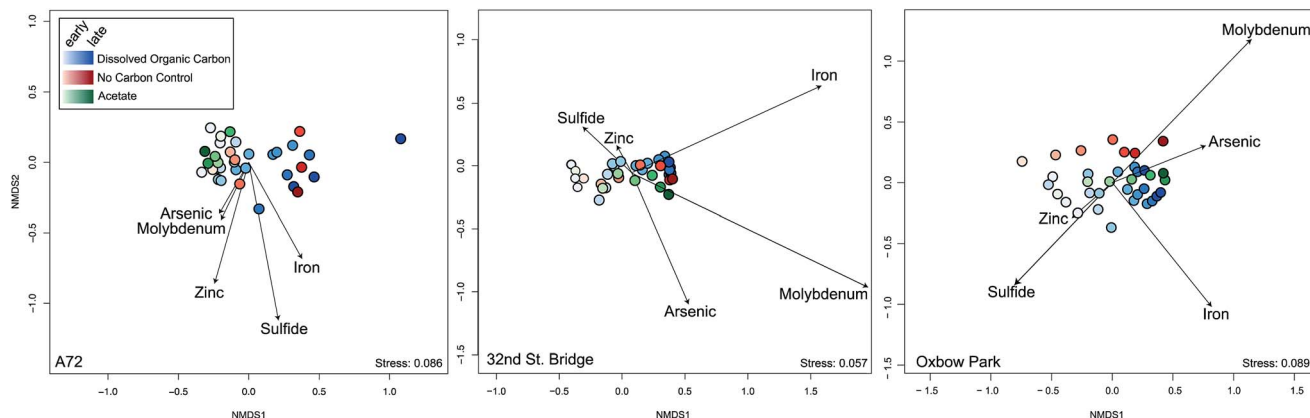
mobilization may be attributed to the presence of the acetate anion in the solution, which is known to accelerate nucleation kinetics of ZnS by reducing the nucleation barrier.[18,19] Although ZnS (sphalerite) was not observed via XRD, quantities formed from the millimolar concentrations of S^{2-} and ppm concentrations of aqueous Zn would likely have been either below the XRD detection limit or poorly crystalline. The lack of additional metal mobilization may be due to the large remaining sedimentary sorbent pool (e.g., Fe-oxyhydroxides, illites) that could rapidly re-adsorb mobilized species. Additionally, the metal biogeochemistry may be influenced by the cation exchange capacity of the remaining clay minerals as well as the competitive adsorption sequence of the cations identified in this study.
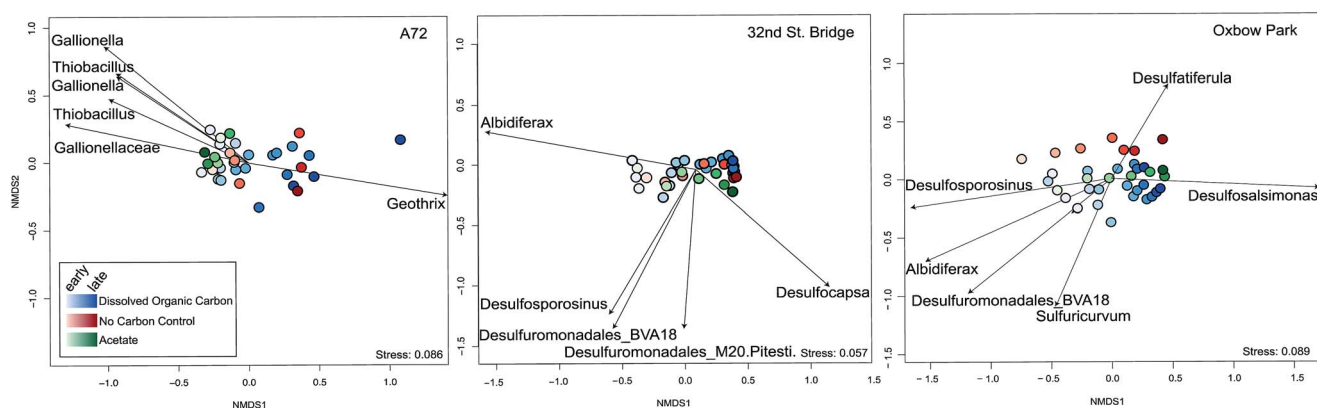
Fig. 5 Non-metric multidimensional scaling (NMDS) plots of microbial community data (16S rRNA genes) for each location; A72 (left), 32nd St. Bridge (center), and Oxbow Park (right). Distances between plotted points are directly linked to their Bray–Curtis dissimilarity. Vectors indicate geochemical parameters driving the shifts in microbial communities. Proximity to vectors indicates correlation and vector length indicates magnitude of influence. DOC = dissolved organic carbon.

Fig. 6 Non-metric multidimensional scaling (NMDS) plots of microbial community data (16S rRNA genes) for each location; A72 (left), 32nd St. Bridge (center), and Oxbow Park (right). Distances between plotted points are directly linked to their Bray–Curtis dissimilarity. Vectors represent dominant inferred Fe- and S-oxidizing and Fe-reducing OTUs driving the overall shifts in microbial communities, as inferred from SIMPER analyses. Proximity to vectors indicates correlation and vector length indicates magnitude of influence. DOC = dissolved organic carbon.

microcosm) is directly related to their Bray–Curtis dissimilarity—a statistic used to quantify the difference between the structure of two or more communities.[29] Vectors overlying the plotted points indicate geochemical parameters (Fig. 5) and putative Fe- and S-oxidizing and Fe-reducing OTUs (Fig. 6) which drive the shifts observed in microbial communities. Proximity to vectors indicates correlation while vector length indicates magnitude of influence. Within microcosm experiments, these same analyses revealed progressive changes in community structure over the incubation period (Fig. 5 and 6). 16S rRNA gene analyses revealed clear, statistically significant differences in microbial community structures between the A72 location, and the Oxbow Park and 32nd St. Bridge locations, reflecting spatial and mineralogical variability across these sites (ANOSIM R scores; A72/Oxbow = 0.9976, A72/32nd St. Bridge = 0.9991, Oxbow/32nd St. Bridge = 0.6034). OTUs matching putative Fe- and S-oxidizing chemolithoautotrophs (*e.g.*, *Thiobacillus*,[30] *Gallionella*[31]) were initially more abundant in sediments from the A72 location, potentially respiring on the large

pool of bioavailable Fe substrates.[32] *Via* SIMPER (simper, vegan package v.2.4-2 (ref. 29)) analyses, these groups were responsible for much of the dissimilarity (~5%) between microbial communities at initial and later time points. Also contributing to this dissimilarity were OTUs matching potential Fe-reducing *Geothrix*-like microorganisms (~2%) that were instead more abundant at later time points and were presumably stimulated by reducing conditions. The enrichment of these groups may at least partially account for increases in Fe^{2+} during the incubation. For the 32nd St. Bridge samples, OTUs with poor taxonomic resolution within the *Deltaproteobacteria* (*e.g.*, *Desulfobacteraceae*, *Desulfobulbaceae*) were more abundant at mid and later time points (Fig. 6), and accounted for much of the dissimilarity between initial and later samples (~6.5%). Similar OTUs were found to partially account for the dissimilarity (~6.8%) between samples in the Oxbow Park microcosms (ESI†). Microbially-enhanced dissolution of minerals such as jarosite by Fe^{3+}- and SO_4^{2-} reducers has been demonstrated to play a major role in the mobilization of metals (*i.e.*, As, Pb) across changing

environmental conditions (*e.g.*, pH, redox).[23,24] Given that many microbial groups within the *Deltaproteobacteria* are responsible for metal and SO_4^{2-} reduction, these OTUs may have been catalyzing similar processes in these Animas River sediments.

Summary and conclusions

Differences in sediment mineralogy and adsorbed metal loadings were strongly linked to sampling locations and proximity to metal contaminant point sources. Results suggest that reductive microbial metabolisms will likely play a significant role in mobilizing adsorbed metal pools following burial of riverbed sediments and the accompanying onset of anoxic conditions. The site-specific nature of metal release may be linked to different reductive metabolisms, with Fe-reduction driving dissolution of grain coatings and alkalinity increases during SO_4^{2-} reduction offering another mechanism for metal desorption.[24] Given the Fe- and S-rich nature of the Colorado Basin,[3,13] these complex processes represent a challenge for the tracking of mining-impacted biogeochemistry and associated water quality issues, and emphasize the need monitoring efforts that account for the dynamic nature of fluvial systems and their ability to moderate strong spatial and temporal gradients in redox status. These results carry important implications for the role of microbes in the mobilization of sediment associated metal pools across a wide range of environments. As this is one of the few investigations of sediment biogeochemistry in the Animas River watershed following the Gold King Mine spill, this study provides valuable insights into the possible changes and patterns of metal (re) mobilization, particularly in mining-impacted locations.

Acknowledgements

References

1 S. G. Benner, D. W. Blowes, W. D. Gould, R. B. Herbert and C. J. Ptacek, *Environ. Sci. Technol.*, 1999, **33**, 2793–2799.

2 B. Jones, *Integr. Investig. Environ. Eff. Hist. Min. Animas River Watershed, San Juan Cty., Color. Prof. Pap.*, 2008, vol. 1651, pp. 43–55.

3 B. M. A. Mast, P. L. Verplanck, W. G. Wright and D. J. Bove, *Integr. Investig. Environ. Eff. Hist. Min. Animas River Watershed, San Juan Cty., Color. Prof. Pap.*, 2008, vol. 1651, pp. 347–386.

4 M. Gobla, C. Gemperline and L. Stone, Technical Evaluation of the Gold King Mine Incident, *Reclamation: Managing Water in the West*, 2015.

5 R. R. Gadde and H. a. Laitinen, *Anal. Chem.*, 1974, **46**, 2022–2026.

6 C. Petersen, W. Willer and E. Willamowski, *Water, Air, Soil Pollut.*, 1997, **99**, 515–522.

7 S. a. Nagorski and J. N. Moore, *Water Resour. Res.*, 1999, **35**, 3441–3450.

8 V. K. Stucker, K. H. Williams, M. J. Robbins and J. F. Ranville, *Environ. Toxicol. Chem.*, 2013, **32**, 1216–1223.

9 M. F. Schultz, M. M. Benjamin and J. F. Ferguson, *Environ. Sci. Technol.*, 1987, **21**, 863–869.

10 F. S. Islam, A. G. Gault, C. Boothman, D. a. Polya, J. M. Charnock, D. Chatterjee and J. R. Lloyd, *Nature*, 2004, **430**, 68–71.

11 S. G. Benner, C. M. Hansel, B. W. Wielinga, T. M. Barber and S. Fendorf, *Environ. Sci. Technol.*, 2002, **36**, 1705–1711.

12 M. Taillefert, A. B. Bono and G. W. Luther, *Environ. Sci. Technol.*, 2000, **34**, 2169–2177.

13 S. J. Morrison, C. S. Goodknight, A. D. Tigar, R. P. Bush and A. Gil, *Environ. Sci. Technol.*, 2012, **46**, 1379–1387.

14 A. S. Todd, A. H. Manning, P. L. Verplanck, C. Crouch, D. M. Mcknight and R. Dunham, *Environ. Sci. Technol.*, 2012, **46**, 9324–9332.

15 S. Findlay, *Limnol. Oceanogr.*, 1995, **40**, 159–164.

16 A. E. Parada, D. M. Needham and J. A. Fuhrman, *Environ. Microbiol.*, 2015, **18**, 1403–1414.

17 J. G. Caporaso, J. Kuczynski, J. Stombaugh, K. Bittinger, F. D. Bushman, E. K. Costello, N. Fierer, A. G. Peña, J. K. Goodrich, J. I. Gordon, G. a. Huttley, S. T. Kelley, D. Knights, J. E. Koenig, R. E. Ley, C. a. Lozupone, D. Mcdonald, B. D. Muegge, M. Pirrung, J. Reeder, J. R. Sevinsky, P. J. Turnbaugh, W. a. Walters, J. Widmann, T. Yatsunenko, J. Zaneveld and R. Knight, *Nat. Methods*, 2010, **7**, 335–336.

18 A. Celikkaya and M. Akinc, *J. Am. Ceram. Soc.*, 1990, **73**, 245–250.

19 R. Vacassy, S. M. Scholz, J. Dutta, C. J. G. Plummer, R. Houriet and H. Hofmann, *J. Am. Ceram. Soc.*, 1998, **81**, 2699–2705.

20 H. Du, W. Chen, P. Cai, X. Rong, X. Feng and Q. Huang, *Environ. Pollut.*, 2016, **218**, 168–175.

21 M. Bergaya, F. Lagaly and G. Vayer, *Handb. Clay Sci.*, 2006, vol. 1, pp. 979–1001.

22 D. Carroll, *Geol. Soc. Am. Bull.*, 1959, **70**, 70–100.

23 O. Abollino, M. Aceto, M. Malandrino, C. Sarzanini and E. Mentasti, *Water Res.*, 2003, **37**, 1619–1627.

24 N. A. N. Xu, W. Braida and J. Chen, *Soil Sediment Contam.*, 2013, **22**, 912–929.

25 K. H. Williams, P. E. Long, J. a. Davis, M. J. Wilkins, a. L. N'Guessan, C. I. Steefel, L. Yang, D. Newcomer, F. a. Spane, L. J. Kerkhof, L. McGuinness, R. Dayvault and D. R. Lovley, *Geomicrobiol. J.*, 2011, **28**, 519–539.

26 T. P. Vorlicek, M. D. Kahn, Y. Kasuya and G. R. Helz, *Geochim. Cosmochim. Acta*, 2004, **68**, 547–556.

27 L. Rodriguez-Freire, R. Sierra-Alvarez, R. Root, J. Chorover and J. A. Field, *Water Res.*, 2014, **66**, 242–253.

28 J. Oksanen, *Management*, 2008, **1**, 1–10.

29 R. J. Bray and J. T. Curtis, *Ecol. Monogr.*, 1957, **27**, 325–349.

30 I. Suzuki, T. L. Takeuchi, T. D. Yuthasastrakosol and J. K. Oh, *Appl. Environ. Microbiol.*, 1990, **56**, 1620–1626.

31 K. A. Weber, L. A. Achenbach and J. D. Coates, *Nat. Rev. Microbiol.*, 2006, **4**, 752–764.

32 G. Garrity, D. J. Brenner, N. R. Krieg and J. T. Staley, *Bergey's Manual® of Systematic Bacteriology*, Springer, US, Boston, MA, 2005.